Supporting Information

Aggregation-Induced Emission Silence–Mediated Pathogen Detection Using a Rapidly Degradable Nanographene-Embedded Polymersome

Chia-Yi Cheng[1], Eldhose V Varghese[1], Wen-Jyun Wang[1], Chia-Yu Yao[1], Chia-Hsiang Chen[1,2,] and Wei-Peng Li[1,2,3,4,]**

[1]Department of Medicinal and Applied Chemistry, Kaohsiung Medical University, Kaohsiung 807, Taiwan

[2]Department of Medical Research, Kaohsiung Medical University Hospital, Kaohsiung 807, Taiwan

[3]Drug Development and Value Creation Research Center, Kaohsiung Medical University, Kaohsiung 807, Taiwan

[4]Center of Applied Nanomedicine, National Cheng Kung University, Tainan 701, Taiwan

E-mail: chc@kmu.edu.tw (C.H.C.), wpli@kmu.edu.tw (W.P.L)

Keywords: aggregation-induced emission, nanographene, poly(lactic-co-glycolic acid), *Staphylococcus aureus*, *Escherichia coli*, antibiotic

Preparation of nanographene

A total of eight steps were sequentially performed to obtain six precompounds and nanographene (nanoG; Figure S19). Detailed descriptions of each step follow.

*Synthesis of compound **S1***: A dual-neck flask was charged with 4-bromobenzonitrile (4.97 g, 27.3 mmol), PPh_3 (0.17 g,2.5 mol%), $PdCl_2(PPh_3)_2$ (0.96 g, 5 mol%), CuI (0.17 g, 2.5 mol%), and trimethylsilylacetylene (4.05 g, 41.2 mmol). The flask was degassed and filled with nitrogen. A mixture of THF (60 mL) and Et_3N (5.9 mL) was added using a syringe and allowed to react for 16 h at room temperature. A yellow solid appeared, and the residue was treated with $MeOH/K_2CO_3$ for isolation and then purified through column chromatography on silica gel and eluted with CH_2Cl_2-hexane to obtain **S1**, a colorless solid (2.67 g, 77%).

*Synthesis of compound **S2***: A flask was charged with compound **S1** (1 g, 7.87 mmol) and 4-bromobenzonitrile (1.43 g, 7.87 mmol), PPh_3 (41 mg, 0.16 mmol), $Pd(PPh_3)_2Cl_2$ (110 mg, 0.16 mmol), and Et_3N (30 mL). The mixture was stirred for 10 min with Ar bubbling through the solution, and CuI (60 mg, 0.31 mmol) was then added. The mixture was heated to reflux by stirring under nitrogen for 2 h and filtered. The filtrate was purified using column chromatography on silica gel (hexane/CH_2Cl_2, 3:7) to obtain a white solid product (1.3 g, 72%)

*Synthesis of compound **S3***: A solution of 8.0 g (40.0 mmol) of pyrene and 200 mL of tert-butyl chloride was added to 8.0 g (60.0 mmol) of powdered $AlCl_3$ at 0 °C. After the reaction mixture had been stirred at room temperature for 3 h, it was poured into a large amount of ice/water mixture and extracted with CH_2Cl_2 (twice with 250 mL). The combined CH_2Cl_2 extracts were washed with water (twice with 200 mL) and dried with $MgSO_4$, and the solvent was evaporated in vacuum to leave a residue, which was washed with alcohol to yield a colorless solid. The yield was 78%.

*Synthesis of compound **S4***: A solution of compound **S3** (1.6 mmol) in CH_2Cl_2 (6.4 mL) and CH_3CN (6.4 mL) was produced, and $NaIO_4$ (2.8 g, 13.086 mmol), H_2O (8 mL), and $RuCl_3$, xH_2O (0.04 g, 0.192 mmol) were added. The dark brown suspension was heated at 30–40 °C overnight. The reaction mixture was poured into 500 mL of water and extracted with CH_2Cl_2. The combined extracts were washed with water and brine and dried over anhydrous $MgSO_4$, and the solvent was evaporated in vacuo. The crude product was purified through column chromatography to produce the desired compound, a bright orange crystal, in yield of 40%.

*Synthesis of compound **S5***: Iron pentacarbonyl (0.92 mL, 6.83 mmol) was added to a refluxing mixture of 4-*tert* butyl benzyl bromide (2.414 g, 13.14 mmol), sodium hydroxide (2.27 g), benzyltriethylammonium chloride (0.1 g), deionized water (1.3 mL), and dichloromethane (31.5 mL) under a nitrogen atmosphere. The reaction mixture was refluxed with vigorous stirring overnight and extracted with CH_2Cl_2 (twice with 250 mL). The combined CH_2Cl_2 extracts were washed with water (twice with 200 mL) and dried over magnesium sulfate, and the solvent was evaporated under vacuum. The resulting solid was purified by chromatography on silica gel with a mixture of dichloromethane and petroleum ether (3:1) as the eluent. The yield was 65%.

*Synthesis of compound **S6**:* To a suspension of 2,7-di-tert-butyl-pyrene-4,5,9,10-tetraone (118 mg, 0.32 mmol) and 1,3-bis(4-tert butylphenyl) propan-2-one (204 mg, 0.68 mmol) in dry ethanol (65 mL), DBU (0.18 mL, 1.21 mmol) was added dropwise under argon atmosphere. The mixture was stirred for 40 min at 78 °C. The formed solid was collected through vacuum filtration, washed with cold ethanol (twice with 2 mL), and dried under vacuum to yield a pale green solid. The yield was 70%.

Synthesis of compound NanoG: Compound **S6** (500 mg, 0.528 mmol) and Compound **S2** (250 mg, 1.05 mmol) were added to a dry Schlenk flask equipped with a magnetic stir bar, and 2 mL of diphenylether was added to the flask. The reaction mixture was refluxed for 6 h at 260 °C. The crude product was subjected to column chromatography (DCM/hexane = 2:3 as an eluent). The yield of nanoG was 38%.

Table S1. Nanoparticle-based AIE biosensors for pathogenic bacteria detection.

Types	Materials	Pagthogens	Detection method	LOD	References
Nanoparticle-based biosensors	MNP-2nd DNA probe/target DNA/1st DNA probe-Au-NPs-barcode DNA	*Salmonella*	Fluorescence	1 ng/mL	[1]
	Dye-doped silica NPs	*E. coli* O157:H7	Flow cytometry	1 CFU/mL	[2]
	PGNF	*E. coli*	Electrochemistry	10 CFU/mL	[3]
	GQD-AuNP	*Staphylococcus aureus*	Fluorescence	1 nM	[4]
	Tyr/MNPs-CNTs/GCE	*E. coli*	FIA system	10 CFU/mL	[5]
	MNP-SMCC-DNA $probe_3$-target DNA Fluorescence DNA $probe_2$-AuNP-DNA $probe_1$	*Shigella* species	Fluorescence	10^2 CFU/mL	[6]
	FDNPs	*E. coli*	Fluorescence	1.1×10^5 CFU/μL	[7]
AIE sensors	TPE-DNA@GO	SARS-CoV-2	AIE recovery	Ct value of 20	[8]
	GSH-AuAg NCs	*Baumannii*	AIE silence	2.3×10^3 CFU/mL	[9]
	MSN-PGEDA-CB[7]-TPE	*Staphylococcus aureus, E. coli*	AIE silence	2.5×10^6 CFU/mL	[10]
	NPGHP	*E.coli, Pseudomonas aeruginosa, Staphylococcus aureus, Bacillus subtilis*	AIE effect	1×10^4 CFU/mL	[11]
	NanoGs-embedded PLGA polymersome	Methicillin-resistant *Staphylococcus aureus, E. coli*	AIE silence	2.709×10^8 CFU/mL	This work

MNP: magnetic nanoparticle; DNA: deoxyribonucleic acid; NP: nanoparticle; PGNF: Pt-nanoparticle-coated gold nanoporous film; GQD: graphene quantum dot; Tyr: tyrosinase; CNT: carbon nanotube; GCE: glassy carbon electrode; SMCC: sulfosuccinimidyl 4-nmaleimidomethyl cyclohexane-1- carboxylate; FDNP: fluorescent dextran nanoparticle; TPE: tetraphenylethene; GO: graphene oxide nanosheet; GSH: L-glutathione; NC: nanocluster; MSN: mesoporous silica nanoparticle; PGEDA: ethylenediamine-modified polyglycerol methacrylate; CB[7]: cucurbit[7]uril; NPGHP: nanoengineered peptide-grafted hyperbranched polymer; FIA: flow injection assay.

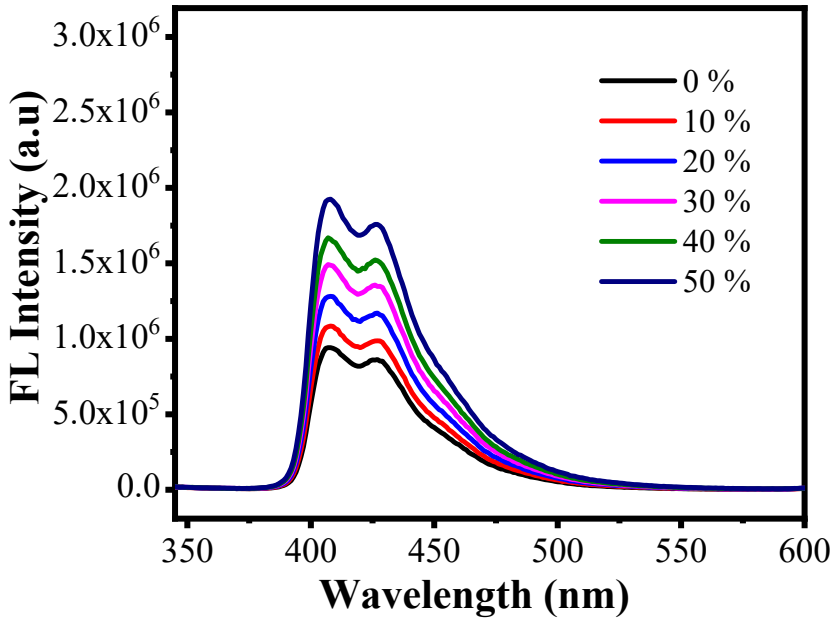

Figure S1. Fluorescent spectra of nanoG dispersed in cosolvent at various water–THF ratios. Increasing the THF content increased the AIE effect of the nanoG.

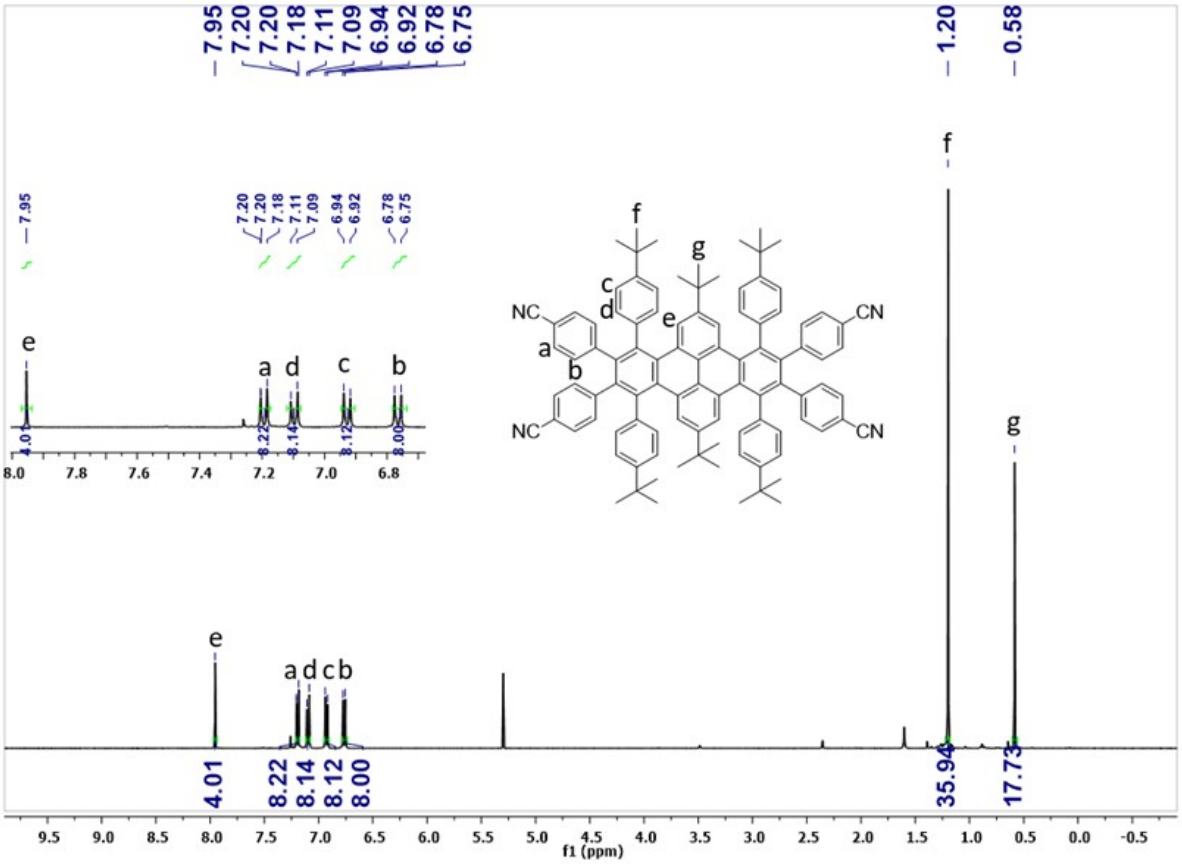

Figure S2. ^{1}H NMR spectrum of nanoG in $CDCl_3$ (400 MHz, 298 K).

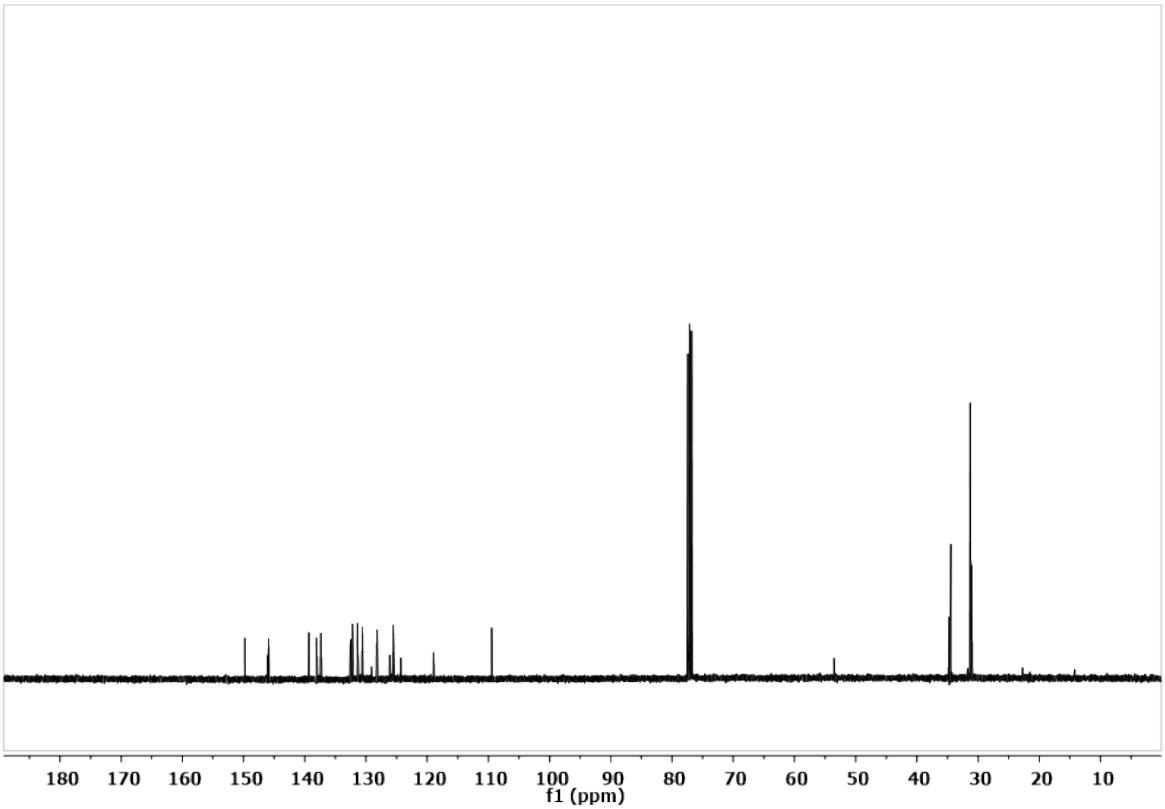

Figure S3. ^{13}C NMR spectrum of nanoG in $CDCl_3$ (400 MHz, 298 K).

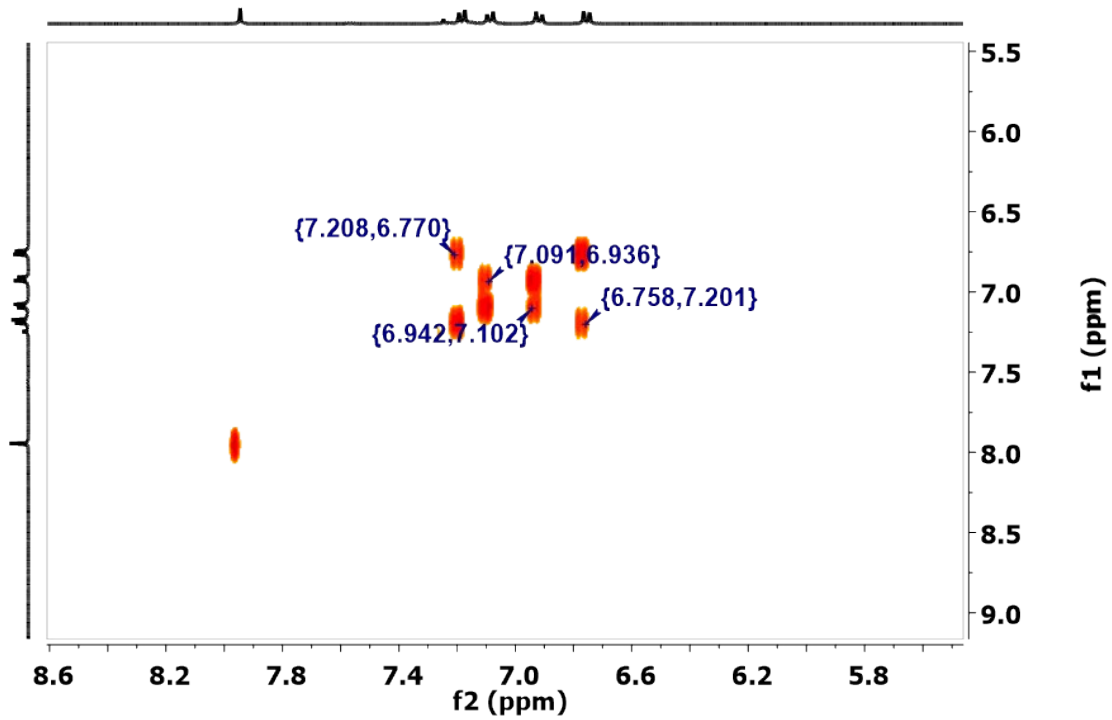

Figure S4. ^{1}H-^{1}H COSY spectrum of nanoG in $CDCl_3$ (400 MHz, 298 K).

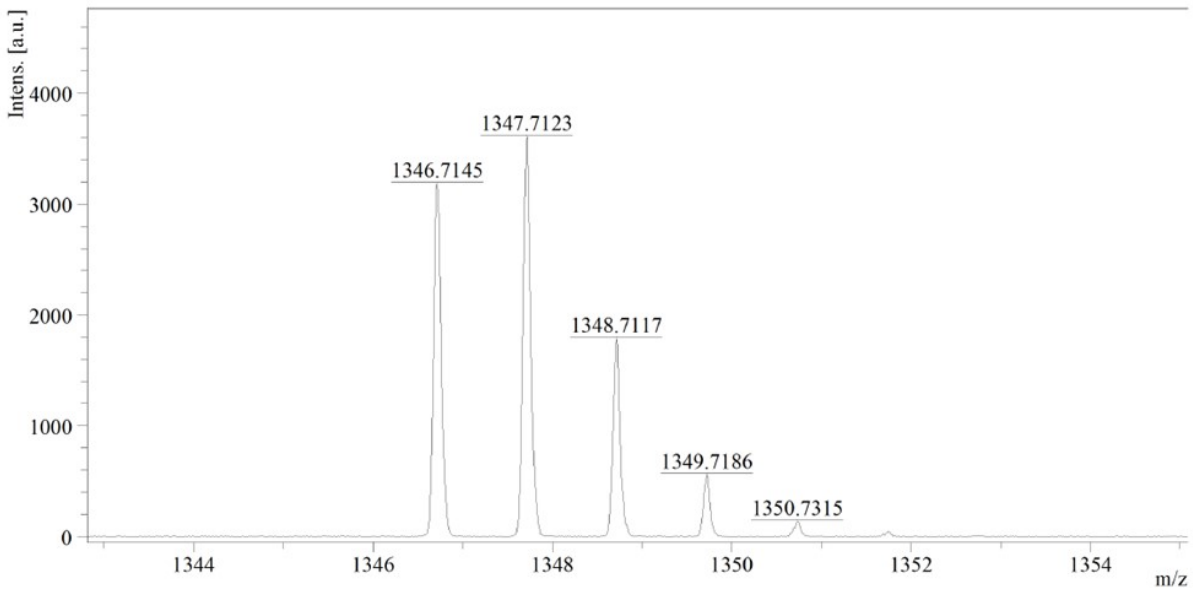

Figure S5. High-resolution mass spectrum of nanoG.

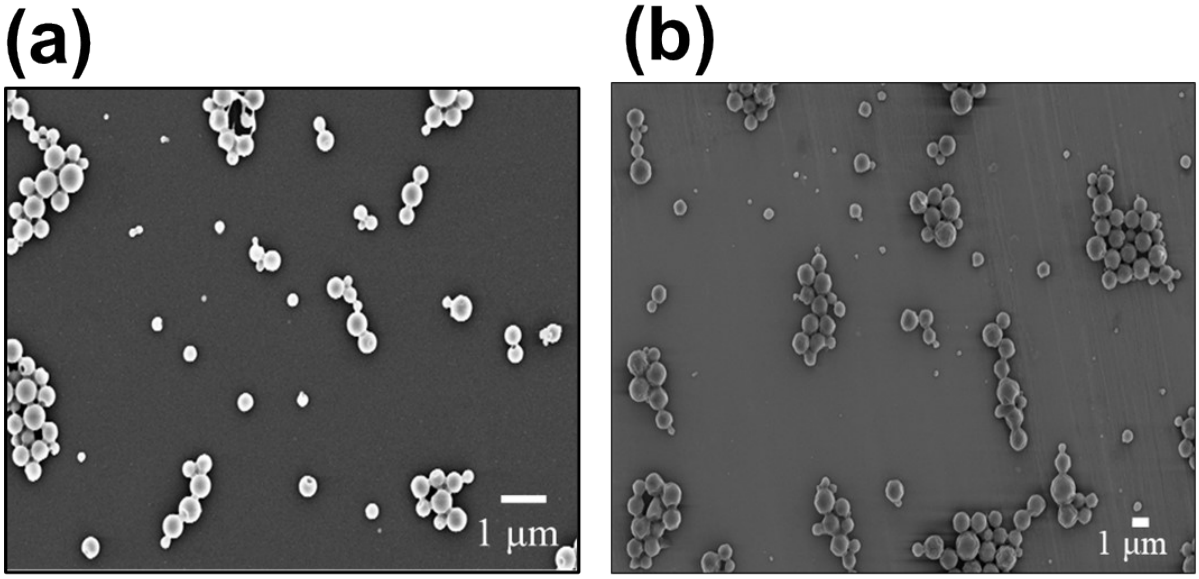

Figure S6. SEM images of (c) PLGA and (d) nanoG-embedded PLGA polymersomes.

	Zeta potential (mV)	Size (nm)
PLGA	**-15.43**	**825**
NanoG-PLGA	**-19.92**	**865**

Figure S7. Dynamic light scattering and zeta potential of PLGA polymersome with and without nanoG.

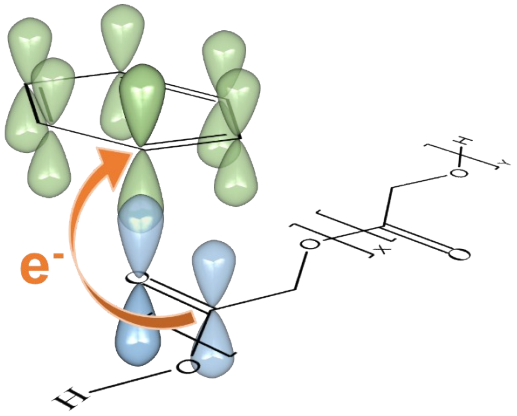

Figure S8. Illustration of the π–π interaction between aromatic benzene and the carboxylic group of PLGA, which enables electron donation from PLGA to the aromatic-ring-rich nanoG.

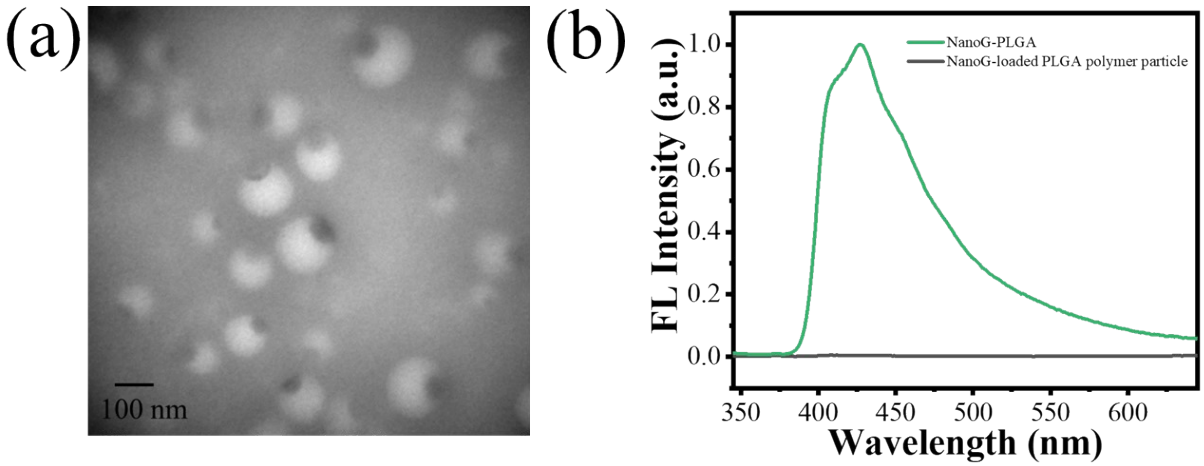

Figure S9. (a) The TEM image of nanoG-loaded PLGA polymer particle prepared by single emulsion method. The dark contrast area in the spheres indicated the nanoG aggregation in the polymer particle. (b) Fluorescence spectra of nanoG-embedded PLGA polymersomes and nanoG-loaded PLGA polymer particles upon excitation at 330 nm.

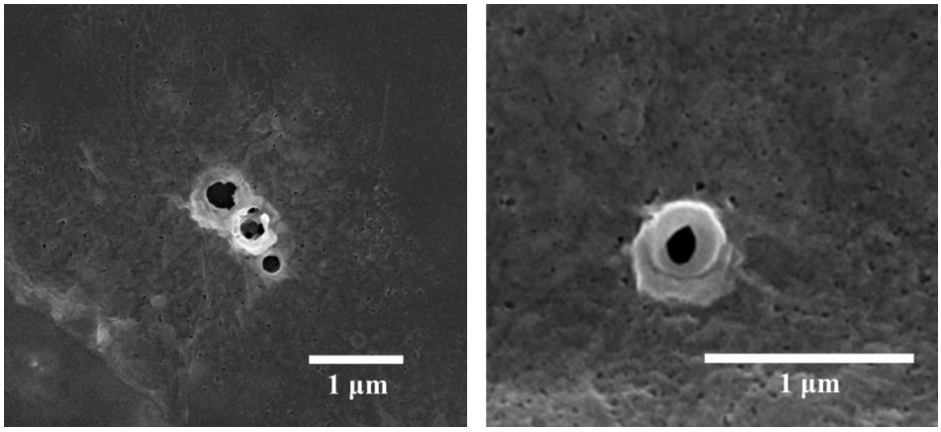

Figure S10. SEM images of nanoG-embedded PLGA polymersomes incubated with bacteria for 24h.

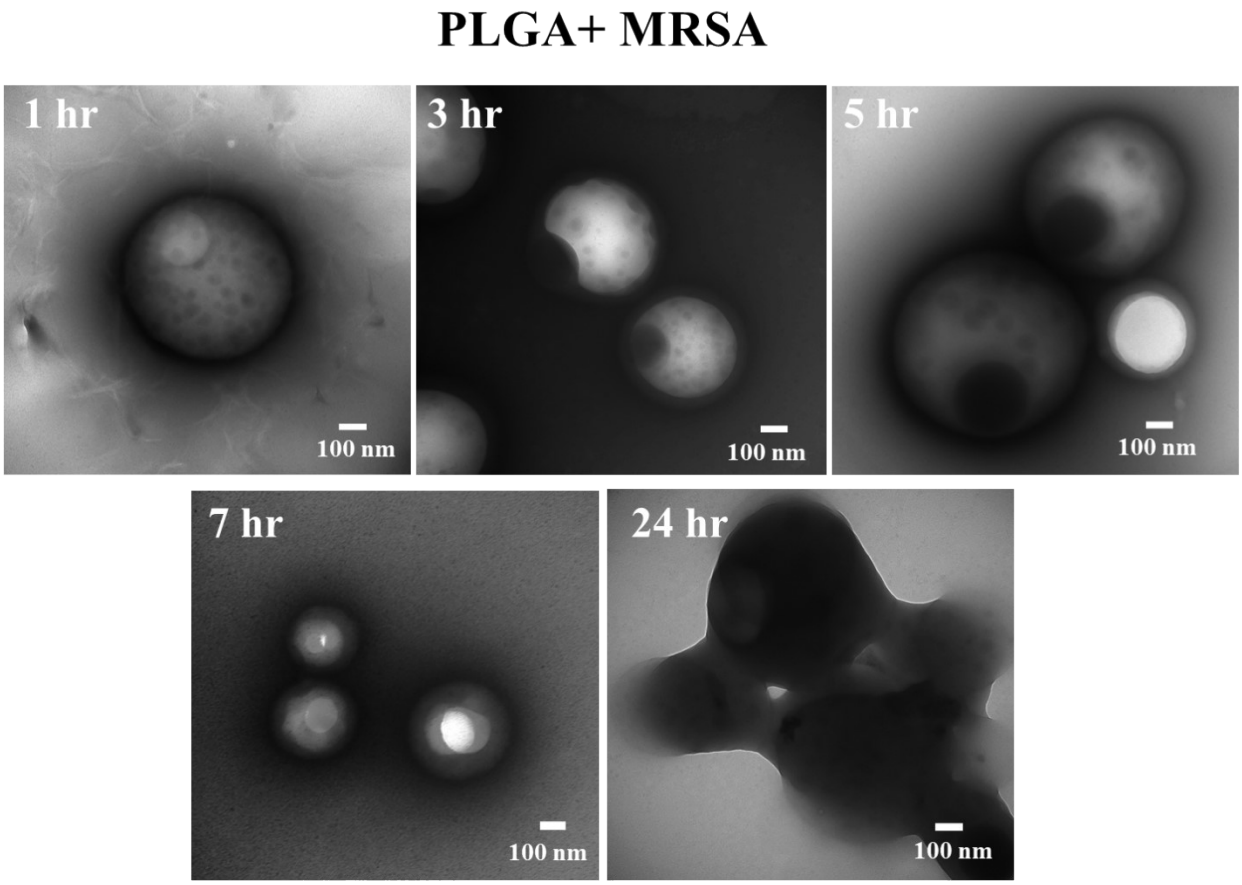

Figure S11. TEM images of PLGA polymersome incubated with MRSA at 6.7×10^7 CFU/mL at 37 °C for various incubation times (0, 1, 3, 5, or 24 h).

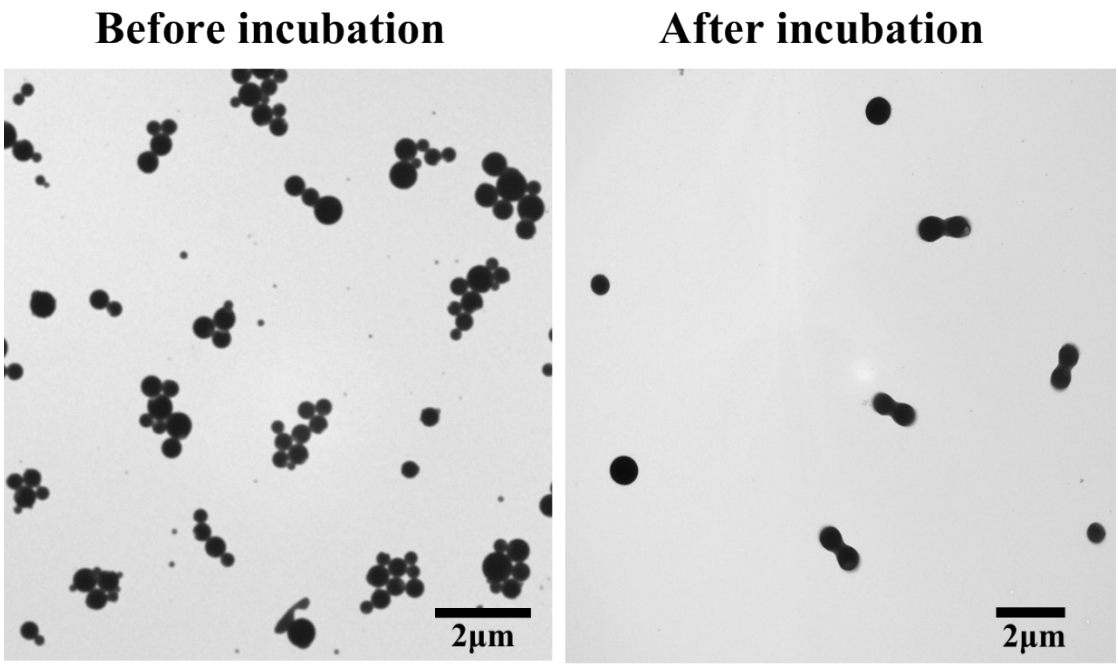

Figure S12. TEM images of nanoG-embedded PLGA polymersome dispersed in cell-free medium at 37 °C for 24 h.

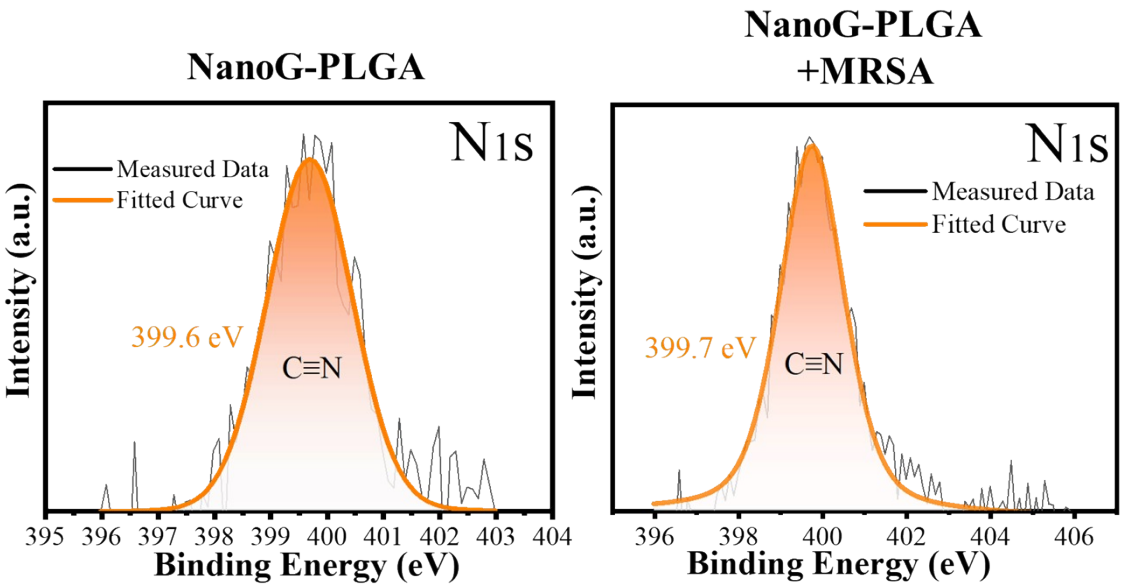

Figure S13. XPS analysis results of nanoG-embedded PLGA polymersome before and after incubation with MRSA in 6.7×10^7 CFU/mL at 37 °C for 24 h.

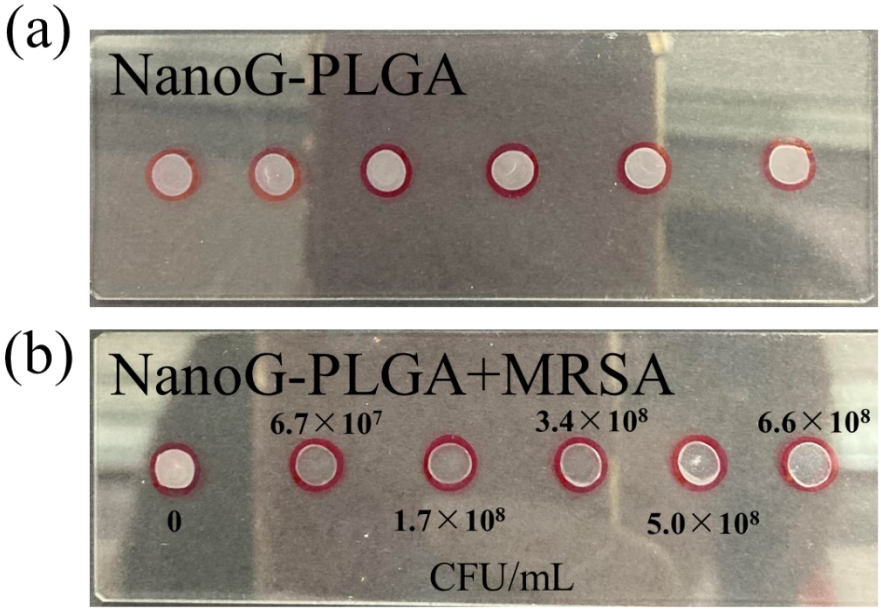

Figure S14. Photographs of AIE thin films without UV light exposure. (a) Total of 10 μL of nanoG-embedded PLGA polymersome was deposited on a glass slide to form AIE thin-film test zones (marked by red circles). (b) AIE thin-film test zones after dropping 10 μL of buffer solution containing MRSA at different concentrations (6.7×10^7, 1.7×10^8, 3.4×10^8, 5.0×10^8, 6.7×10^8 CFU/mL).

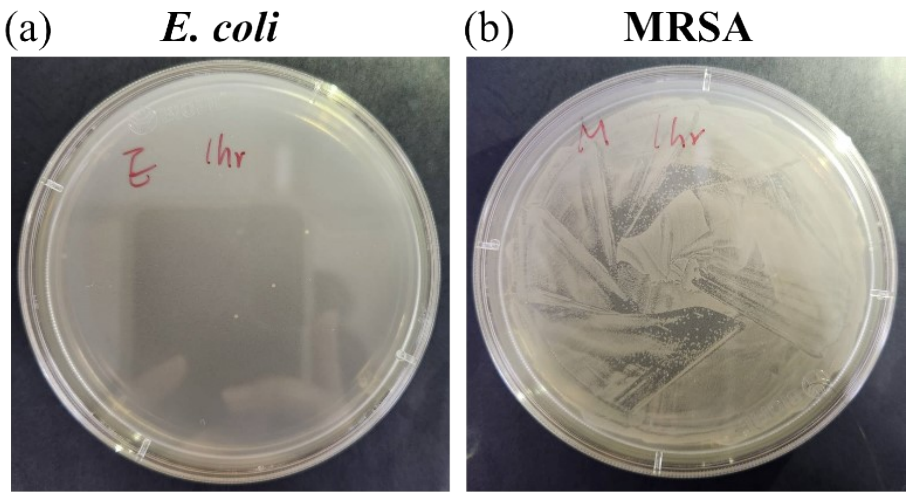

Figure S15. Colony assays of (a) *E. coli* and (b) MRSA with kanamycin (9 μg/mL). A total of 100 μL of the bacterial solution containing antibiotic was added to an LB agar plate and incubated at 37 °C for 24 h.

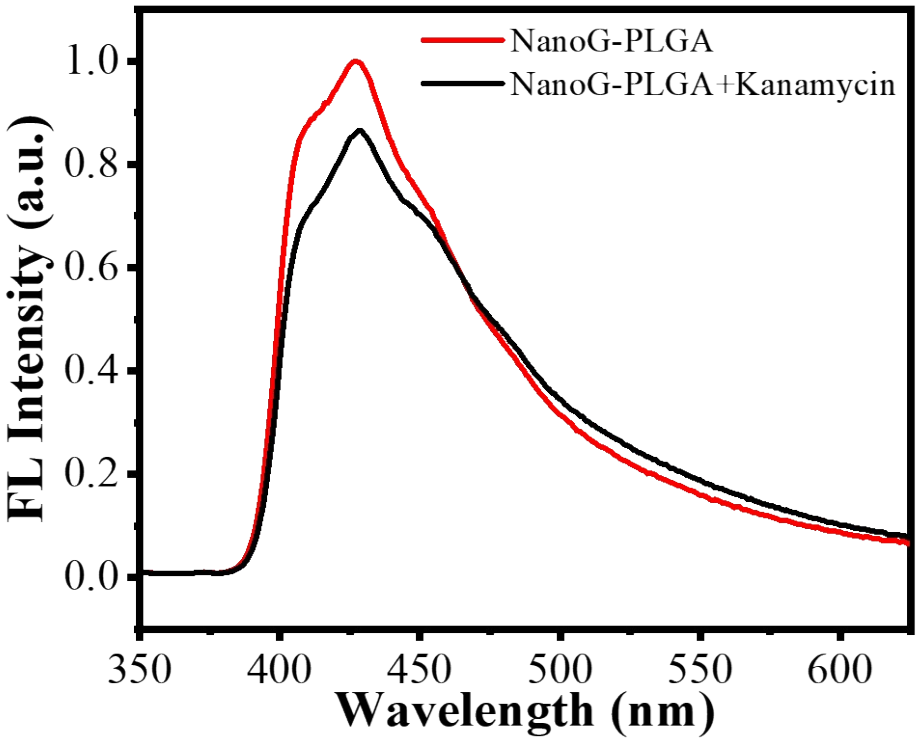

Figure S16. Fluorescence spectra of nanoG-embedded PLGA polymersome before and after incubation with kanamycin at 37 °C for 1 h.

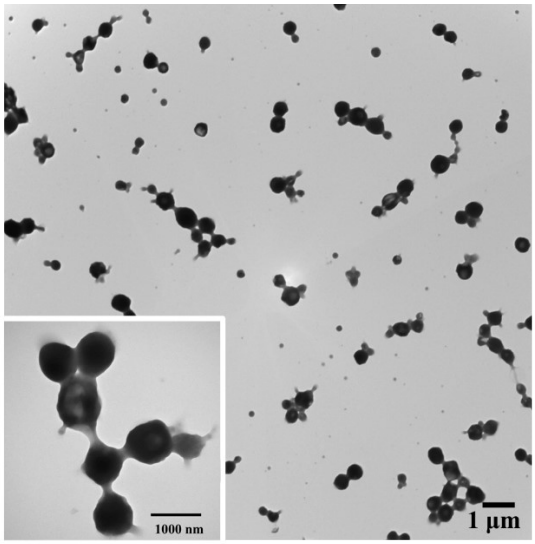

Figure S17. TEM image of kanamycin-loaded nanoG-embedded PLGA polymersome.

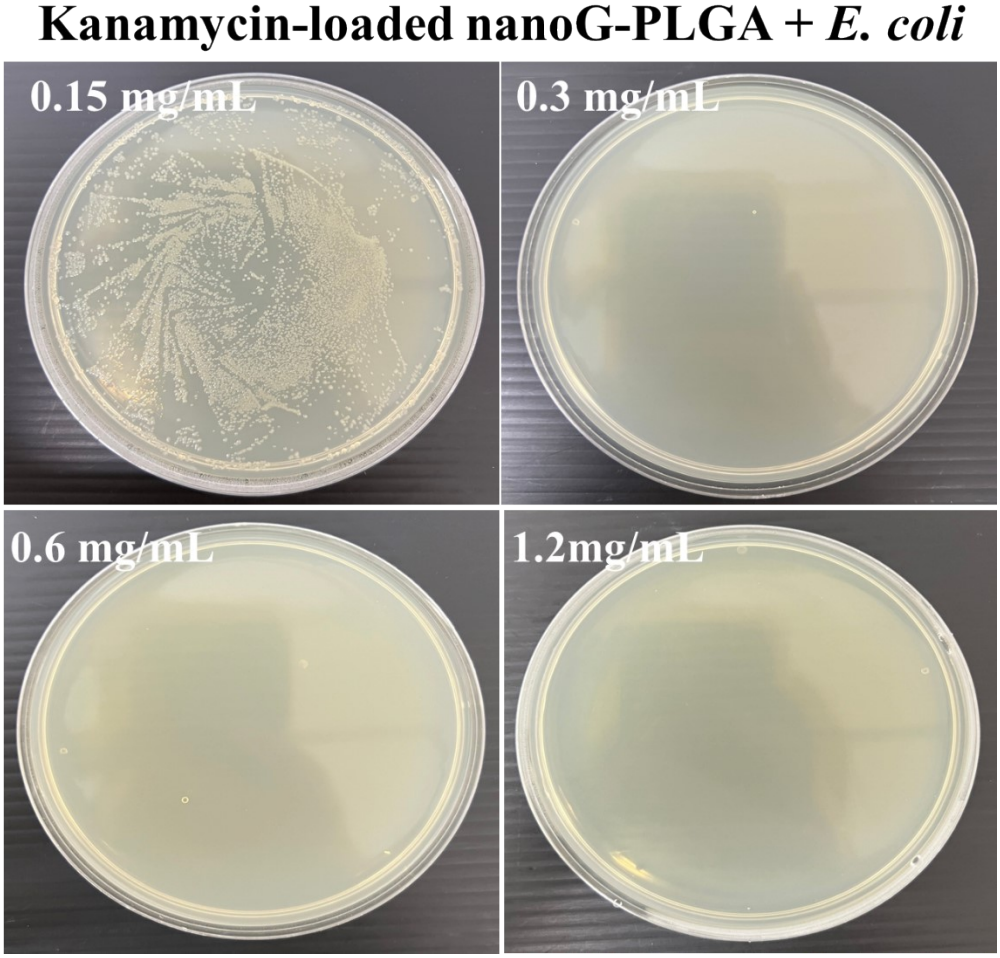

Figure S18. Colony assay of *E. coli* with kanamycin-loaded nanoG-PLGA at different concentrations. A total of 100 μL of the bacterial solution containing antibiotic was added to an LB agar plate and incubated at 37 °C for 24 h.

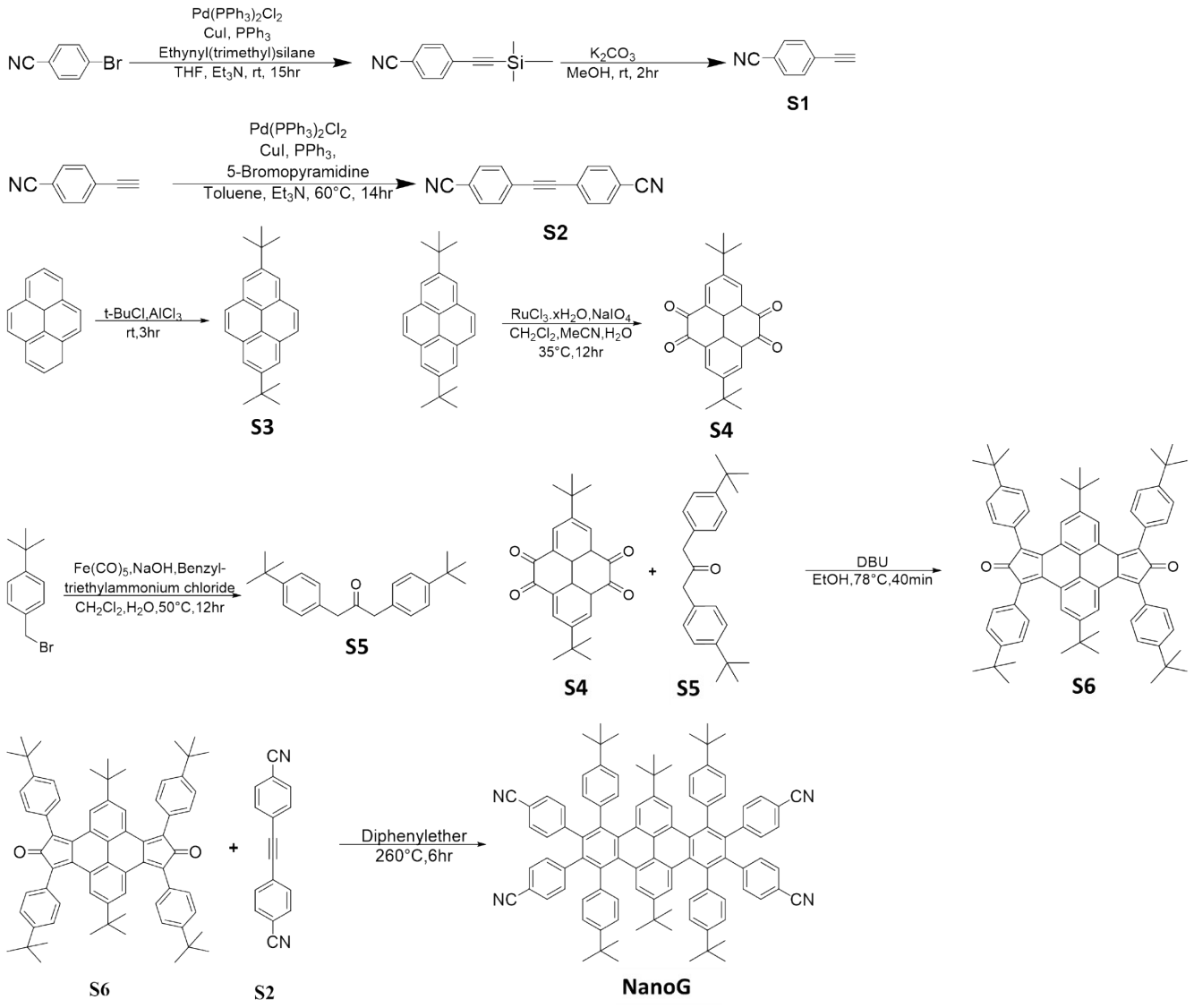

Figure S19. NanoG synthesis procedure.

References:

[1] D. Zhang, D. J. Carr and E. C. Alocilja, *Biosens. Bioelectron.*, 2009, **24**, 1377-1381.

[2] S. J. Mechery, X. J. Zhao, L. Wang, L. R. Hilliard, A. Munteanu and W. Tan, Chem.

Asian J., 2006, **1**, 384-390.
[3] Q. Yang, Y. Liang, T. Zhou, G. Shi and L. Jin, Electrochem. commun., 2009, **11**, 893-896.
[4] J. Shi, C. Chan, Y. Pang, W. Ye, F. Tian, J. Lyu, Y. Zhang and M. Yang, Biosens. Bioelectron., 2015, **67**, 595-600.
[5] Y. Cheng, Y. Liu, J. Huang, K. Li, Y. Xian, W. Zhang and L. Jin, Electrochim. Acta, 2009, **54**, 2588-2594.
[6] N. Elahi, M. Kamali, M. H. Baghersad and B. Amini, Mater. Sci. Eng. C, 2019, **105**, 110113.
[7] J. H. Lee, J. S. Ryu, Y. K. Kang, H. Lee and H. J. Chung, Adv. Funct. Mater., 2021, **31**, 2007993.
[8] Q. Zhang, B. Yin, J. Hao, L. Ma, Y. Huang, X. Shao, C. Li, Z. Chu, C. Yi and S. H. D. Wong, Aggregate, 2023, **4**, e195.
[9] Y. Zheng, X. Wang and H. Jiang, Sens. Actuators. B Chem., 2018, 277, 388-393.
[10] Q. Li, Y. Wu, H. Lu, X. Wu, S. Chen, N. Song, Y.-W. Yang and H. Gao, ACS Appl. Mater. Interfaces., 2017, 9, 10180-10189.
[11] J. Zhao, Z. Dong, H. Cui, H. Jin and C. Wang, ACS Appl. Mater. Interfaces., 2018, 10, 42058-42067.